

Probabilistic map of blood flow distribution in the brain from the internal carotid artery

Jae Sung Lee, Dong Soo Lee,* Yu Kyeong Kim, Jinsu Kim, Ho Young Lee, Sang Kun Lee, June-Key Chung, and Myung Chul Lee

Departments of Nuclear Medicine and Neurology, Seoul National University, College of Medicine, Seoul 110-744, Korea

Received 9 April 2004; revised 19 July 2004; accepted 21 July 2004

Brain single photon emission computed tomographic (SPECT) images acquired after injecting Tc-99m-HMPAO into the internal carotid artery (ICA) during an intracarotid amobarbital procedure (IAP SPECT) provide anatomical information on the blood flow distribution from the ICA. In this study, probabilistic maps of the distribution of blood supply from the ICA were developed using the IAP SPECT images. Twenty-two sets of basal and IAP SPECT were collected from an existing database. IAP SPECT images were coregistered to basal SPECT images, and spatial normalization parameters used for basal SPECT images were reapplied to IAP SPECT for anatomical standardization. Pixel counts of IAP SPECT images were then normalized, and the probabilistic map of cerebral perfusion distribution (perfusion probabilistic map) for each hemisphere was determined by averaging the spatial/count-normalized IAP SPECT images. Population-based probabilistic maps representing the extent of ICA territory (extent probabilistic map) were also composed by averaging the binary images obtained by thresholding the spatially normalized IAP SPECT images. The probabilistic maps were used to quantify cerebral perfusion and reserve change after arterial bypass surgery in 10 patients with ICA stenosis. In the probabilistic maps, blood supply from the ICA was found to be most likely in the dorsolateral frontal lobe, the anterosuperior portion of the temporal lobe, and in the frontoparietal area. Of the subcortical regions, the striatum was found to be most likely to derive its blood supply from ICA. In patients with cerebral occlusive disease, improvements in basal perfusion and perfusion reserve in the bypass-grafted ICA territory were well identified and were increased by 6.2% and 4.6%, respectively, on average. The probabilistic maps developed in this study illustrate the perfusion distribution and extent of vascular territory for ICA and would be useful for objective evaluations of perfusion status in cerebrovascular disease.

© 2004 Elsevier Inc. All rights reserved.

Keywords: Blood flow; Internal carotid artery; SPECT

* Corresponding author. Department of Nuclear Medicine, Seoul National University College of Medicine, 28 Yungun-Dong, Chongno-Ku, Seoul 110-799, Korea. Fax: +82 2 766 9083.

E-mail address: dsl@palza.snu.ac.kr (D.S. Lee).

Available online on ScienceDirect (www.sciencedirect.com).

Introduction

Population-based structural and functional maps of the brain provide effective tools for the analysis and interpretation of complex and individually variable brain data (Toga and Thompson, 2001). Probabilistic maps of brain structures based on magnetic resonance image (MRI) data or cytoarchitectonic data have been previously developed and applied to a variety of research areas in neuroscience and medicine (Amunts and Zilles, 2001; Evans et al., 1993; Mazziotta et al., 1995). These applications include the fully automated segmentation of brain MRI and its application to partial volume correction in positron emission tomography (PET) (Collins et al., 1995; Rousset et al., 1998). The regional uptake of radiotracers in PET and in single photon emission computed tomographic (SPECT) images can be quantified by averaging regional intensities, which are weighted using the probabilistic maps of certain brain regions after they have been spatially normalized into the standardized coordinates (Kang et al., 2001). PET and SPECT images have been quantified using the spatial normalization techniques and probabilistic maps to investigate metabolic and perfusion abnormalities in epilepsy patients, age-related alternations in cerebral glucose metabolism, and functional connectivity in hearing disorders (Kang et al., 2003; Lee et al., 2001, 2002). The interpretation of statistical analyses performed in standard brain space is also supported by user-interactive tools designed to assess probabilistic anatomical localizations (Kim et al., 2002; Lancaster et al., 2000).

In addition to anatomical, functional, and cytoarchitectonical probabilistic maps, population-based probabilistic maps of the cerebrovascular system would also be another important tool for medical and scientific purposes. From the medical aspect, cerebrovascular probabilistic maps appear to be more applicable than any other probabilistic maps since they can be applied to numerous basic and clinical investigations related to cerebrovascular disease. The quantification of regional cerebral perfusion in the internal carotid artery (ICA) territory is especially important because the ICA supplies blood to substantial parts of the brain and is the vessel most frequently involved in major cerebrovascular

diseases (Bamford et al., 1991; Johansson et al., 2000; Mead et al., 1998).

Several perfusion imaging techniques have been used to assess the effects of revascularization and regional perfusion status in cases of acute or chronic cerebrovascular occlusive disease. Contrast angiography provides anatomical information about stenosis or new blood vessel formation after bypass surgery; however, sometimes it cannot directly provide information about tissue perfusion. Accordingly, functional images representing cerebral perfusion have been developed, which include perfusion weighted or diffusion-weighted MRI (PWI or DWI), perfusion SPECT, and PET (Baird et al., 1994, 1997; Camargo, 2001). Perfusion SPECT is the best established of these modalities, and its use is increasing (Camargo, 2001; Giubilei et al., 1990; Laloux et al., 1995; Watanabe et al., 1999). Thus, the development of probabilistic maps of the ICA territory based on perfusion images has been encouraged. These probability maps might obviate the need of invasive study to delineate ICA territory in individual studies for the clinical routine examination of patients. Brain PET or SPECT imaging following the direct injection of radiotracer for perfusion assessment into the unilateral ICA via an arterial catheter permits the acquisition of anatomical information about the blood supply from the ICA. In addition, such radiotracers should have high extraction fractions so that it can be substantially extracted after its first pass to prevent it reaching other areas after recirculation. However, such imaging studies with invasive catheterization cannot be conducted in healthy volunteers because of the risks of infection, stroke, and intracerebral hemorrhage associated with catheterizing arterial vessels.

Therefore, in this study, we used retrospective brain SPECT images, which were acquired after injecting Tc-99m-HMPAO into the ICA during an intracarotid amobarbital procedure in epilepsy patients (IAP SPECT or Wada SPECT) (Fig. 1). This procedure was performed preoperatively to predict postoperative memory and language deficit after unilateral temporal lobectomy (Kim et al., 1999, 2000). One of the technical challenges associated with generating a probabilistic map of the ICA territory using IAP SPECT images was the anatomical standardization of these images since a standard IAP SPECT template was unavailable. Moreover, anatomical information for the standardization of brain was

insufficient in IAP SPECT because radiotracer reaches limited brain areas in IAP SPECT images. In this paper, we present procedures for the anatomical standardization of IAP SPECT images and resulting products of probabilistic maps of blood flow distribution from the ICA and include the results of preliminary clinical applications of these probabilistic maps.

Materials and methods

Subjects

Basal interictal SPECT (standard brain SPECT imaging without intervention) and IAP SPECT, data were collected retrospectively from an existing database consisting of scans performed between July 1995 and April 1996 at Seoul National University Hospital. All images were reexamined by two nuclear medicine physicians. Images with poor image quality due to a small injection dose or severe perfusion defect due to anatomical abnormalities were excluded. If any anatomical abnormality other than hippocampal sclerosis was shown on MRI, we excluded the subject too. Twenty-two patients were finally included from 31 patients with temporal lobe epilepsy who underwent basal SPECT and IAP SPECT during this period. There were 11 men and 11 women, of mean age 28.0 ± 10.7 years.

Basal and IAP brain SPECT

Basal and IAP brain SPECT images were acquired using a triple head gamma camera (Prism 3000; Picker International, Cleveland, OH) with a fan-beam collimator. All subjects were placed in a supine position, with their eyes closed, in a quiet room with dimmed lights. Approximately 555 MBq Tc-99m-HMPAO was administered. The energy window was set at 140 keV with a 15% width. One hundred and twenty frames were acquired over 20 s in a step-and-shoot mode. Transaxial images were reconstructed as 64×64 matrixes and filtered using a Metz filter ($\lambda = 1.5 \sim 2.0$). All images were corrected for attenuation using Chang's method (Chang, 1978).

An intracarotid amobarbital procedure (IAP) was performed as part of the presurgical evaluation of the patients who were considered potentially suitable for unilateral temporal lobectomy to prevent postoperative memory and language deficit after resection of the epileptogenic temporal lobe (Kim et al., 1999, 2000). An arterial catheter was placed 5 cm below the intracarotid bifurcation by femoral catheterization. The position of the catheter and the existence of vascular abnormalities were checked by serial angiographic demonstration before the amobarbital procedure. Electroencephalographic (EEG) monitoring was used during the procedure. A mixture of 80 mg of sodium amobarbital and 555 MBq of Tc-99m-HMPAO was injected into the unilateral ICA feeding the presumptive epileptogenic hemisphere (right hemisphere in 15 of 22 patients and left in 7). IAP SPECT was carried out within 3 h of completing the IAP procedure using the same protocol as used for basal SPECT. Since Tc-99m-HMPAO is substantially extracted immediately after direct injection into the ICA (extraction fraction is 0.72 at a cerebral blood flow of $0.59 \text{ ml g}^{-1} \text{ min}^{-1}$) (Lassen et al., 1988), IAP SPECT image was assumed to reflect a snapshot of the cerebral blood flow from the ICA. Fig. 1 is an example of the IAP SPECT image acquired after injecting Tc-99m-HMPAO through the left ICA.

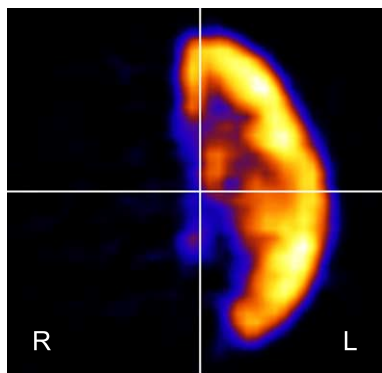


Fig. 1. A transaxial slice of an intracarotid amobarbital brain SPECT image (IAP SPECT), which was acquired after injecting Tc-99m-HMPAO into the left internal carotid artery (ICA) during the intracarotid amobarbital procedure (Wada test) in an epilepsy patients. The IAP SPECT image obtained provides anatomical information about the blood flow distribution from the ICA.

Image registration and anatomical standardization

IAP SPECT image of each individual was coregistered with the corresponding basal SPECT image. The basal SPECT image was then spatially normalized onto the standard Tc-99m-HMPAO SPECT template, and the normalization parameter of the basal SPECT image was then reapplied to the IAP SPECT image.

The SPM99 (Statistical Parametric Mapping 99; Institute of Neurology, University College of London, UK) and FIRE (Functional Image Registration; Seoul National University, Seoul, Korea) programs were used for image registration and for the spatial normalization of the SPECT images (Friston et al., 1995; Lee et al., 2002). IAP SPECT images were registered to basal SPECT images using two different automatic registration algorithms implemented in SPM software, one which minimizes intensity differences and another that maximizes the mutual information between images (Friston et al., 1995; Maes et al., 1997). However, the image registration results obtained using these automatic algorithms were unsatisfactory because of Tc-99m-HMPAO distribution discrepancies in the IAP and basal brain SPECT images.

To correct for these errors, each set of basal and IAP images coregistered by the automatic algorithm was visually inspected, and misalignments were corrected manually by a nuclear medicine physician (YK Kim) using FIRE software (Lee et al., 2002). This software allows interactive rigid body transformation of images with six degrees of freedoms. This program displays three cross-reference views (axial, coronal, and sagittal) of the image, which can be rotated and translated by pushing the control buttons or drawing the lines using mouse. The magnitudes of the rotation angle and the translation distance of the images can be varied from 0.1° to 270° and 0.1 to 270 mm,

respectively. To simplify the manual registration, an analytically composed fusion images of the reference and floating images are displayed with the controllable opacity of the overlaid floating image (Fig. 2) (Foley et al., 1996; Porter and Duff, 1984). A cine display of the fusion image with gradually changing opacity from fully transparent to fully opaque and contours of the reference or floating image overlaid on the other image helped the investigators to examine the correctness of image registration.

Boundaries of the brain cortex and of subcortical structures with high activity (basal ganglia and anterior temporal area) in both images were used as anatomical landmarks for manual registration with the assumption that regional perfusion in the brain areas attributable to the ICA is identical in both the basal and IAP SPECT images. The boundaries of these regions shown in cross-reference views were compared and matched.

After image registration, basal SPECT images were spatially normalized onto the standard SPECT template using SPM99, which contains a standard Tc-99m-HMPAO SPECT template (mean image of 22 normal volunteers). Affine transformations were performed to determine the 12 optimal parameters used to register the brain on the standard template. Small differences, between the transformed image and the template, were removed by the elastic deformation method. This deformation was controlled so that deformation field consisted of a linear combination of predefined smooth basis functions for discrete cosine transformation (Friston et al., 1995). Normalization parameters for basal SPECT images were then reapplied to the IAP SPECT images, which had been registered to the basal SPECT images. Spatially normalized IAP SPECT images were resliced using a sinc interpolation method to a dimension of $79 \times 95 \times 68$ voxels of size $2 \times 2 \times 2$ mm, which are the default output in SPM99.

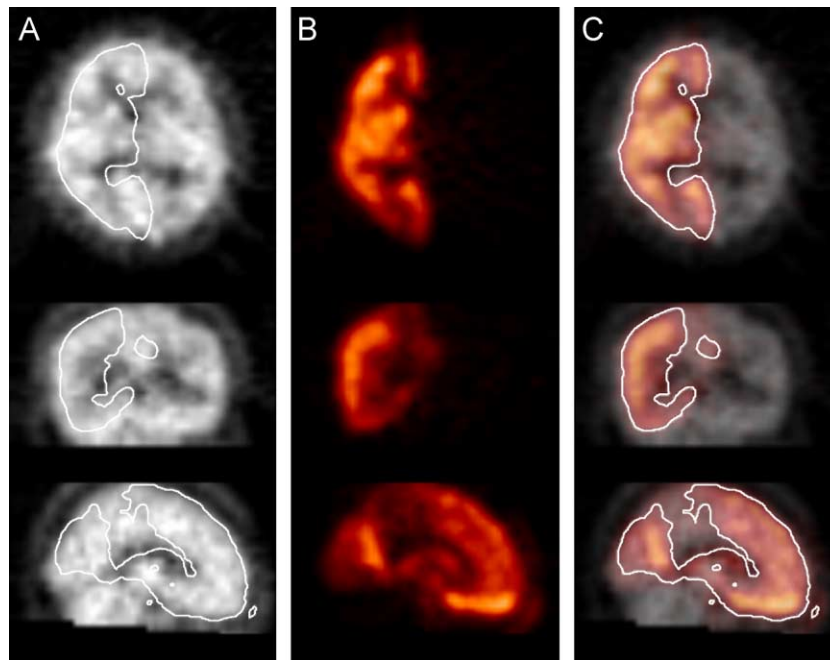


Fig. 2. IAP SPECT images were manually registered to basal SPECT images using FIRE software. (A) Basal SPECT (reference image). (B) IAP SPECT (floating image). (C) Analytically composed fusion image of the reference and floating image. Contour of the floating image overlaid on the reference and fusion image helped users determine the accuracy of the registration between the reference and floating images.

Perfusion probabilistic maps

The pixel values of the spatially normalized IAP SPECT images were normalized with respect to the maximum pixel value in each image (count normalization) to remove the effects of different injection doses and individual differences in the global uptake of Tc-99m-HMPAO into the brain. Since the IAP SPECT images were significantly smoothed by interpolating pixel values during the spatial normalization, a single maximum pixel value was used for the count normalization; this represents the average value of several neighboring pixels in the original image. After the count normalization, perfusion probabilistic maps (mean of IAP SPECT images) were composed by averaging the spatially and count-normalized IAP SPECT images ($n = 15$ for the right ICA map and 7 for the left).

Extent probabilistic maps

Spatially normalized IAP SPECT image of each individual was segmented into ICA territory and others (other regions and background) in the following way. First, a binary mask was generated by thresholding the perfusion probabilistic map; threshold was 90% of the maximum pixel value in the perfusion probabilistic map. Second, spatially normalized IAP SPECT image of each individual was masked with the binary mask and mean pixel value in the masked regions was obtained. And third, each IAP SPECT image was thresholded with 30% of the mean pixel value in the masked regions to generate the binary image representing the ICA territory in each individual brain. The threshold of 30% was used since the cortical boundaries of the resulting binary images, and SPM template showed best match when this threshold was used. The binary images were summed and divided by the number of subjects to obtain the extent probabilistic map of ICA territory for each hemisphere.

Preliminary clinical application

To verify the usefulness of these probabilistic maps, they were used to quantify changes in resting cerebral perfusion and perfusion reserve after arterial bypass surgery in 10 patients (5 women, mean age: 51.0 ± 15.0 years) with ischemic cerebral disease. Four of these 10 patients had ipsilateral proximal middle cerebral artery (MCA) stenosis (1 right side and 3 left), 3 had proximal ipsilateral ICA stenosis (all left side), and the other 3 patients had occlusive lesions at the ICA bifurcation due to Moyamoya disease. These patients underwent superficial temporal artery to middle cerebral artery (STA-MCA) anastomosis surgery. Detailed clinical characteristics and voxel-based analysis of these patients were reported in detail elsewhere (Lee et al., 2004).

Resting cerebral perfusion and perfusion reserve after the intravenous injection of acetazolamide (1 g) were measured by Tc-99m-HMPAO brain SPECT 2 weeks before and 2 weeks after surgery. All four images (resting and post-acetazolamide SPECT before and after surgery) of each individual patient were coregistered and spatially normalized onto the standard brain SPECT template using the SPM99 program. For the spatial normalization of these images, normalization parameters were determined using the resting images and applied to both the resting and post-acetazolamide SPECT images to prevent possible errors in the spatial normalization of the post-acetazolamide images due to decreased activity in ischemic regions. Cerebral perfusion

images were then composed by normalizing each voxel count of the SPECT images with respect to the mean count of the cerebellum. Mean cerebral perfusion in cerebellum was assumed to be $50 \text{ ml min}^{-1} \text{ g}^{-1}$. Probability-weighted mean cerebral perfusion for each hemisphere was calculated by the following equation: $\sum(C_i \times P_i) / \sum P_i$, in which C_i represented for the value of i th voxel in SPECT image and P_i the probability value of i th voxel in ICA extent probabilistic map. Percent change in this mean cerebral perfusion after acetazolamide stress from the resting state was defined as the cerebral perfusion reserve of ICA territory of each hemisphere. The resting perfusions and the perfusion reserves of the patients were compared to those of age-matched normal controls ($n = 20$, 10 women, mean age = 59 ± 5.0 years) whose images were selected from the Tc-99m-HMPAO acetazolamide brain SPECT database at our institution. The resting and post-acetazolamide SPECT images of normal controls were acquired using the same SPECT scanner and study protocols as used for the patients.

Results

Perfusion and extent probabilistic maps

Fig. 3 shows the SPM Tc-99m-HMPAO SPECT template and the spatially normalized basal and IAP SPECT images of the same subject. Spatial normalizations of the basal and IAP SPECT images were successful in all subjects who were included in this study.

Fig. 4 shows the extent probabilistic maps for the vascular territory of left and right ICAs, which are superimposed on a standard TI MRI template. Blood supplied from the ICA reached to the wide brain areas including frontal, inferior parietal, and temporo-occipital regions. The extent of blood supply to the anterior part of brain showed little variability across the individuals: extent probability in this region was almost one. On the contrary, the blood supply to the posterior part of brain including inferior temporal regions, posterior cingulate cortex, and temporo-occipital area was variable according to the individuals: extent probability in this region was 0.4–0.5. Then extent probabilistic maps also showed very low likelihood of blood supply to the medial side of the frontal lobe and superior parietal lobule of contralateral hemisphere.

Figs. 5 and 6 show the perfusion probabilistic maps for the left and right ICAs. They represent the cerebral blood flow rate rather than the extent of vascular territory. In the perfusion probabilistic maps, the arterial blood supply from the ICA in the insular cortex and basal ganglia except for caudate nucleus was largest. The cortical blood from ICA was found to feed a region from the frontal pole to as far as the parietooccipital junction. Of these areas, the anterior part of the lateral temporal lobe (i.e., superior temporal gyrus and the dorsolateral frontal region including the middle and inferior frontal gyrus) were found to have a high likelihood of being supplied by the ICA, whereas the posterior region of the middle temporal gyrus, the inferior temporal gyrus, and the mesial temporal structures showed a low likelihood.

Preliminary clinical application

ICA probability-weighted cerebral perfusion obtained using the extent probability maps reflected well the status of illness in

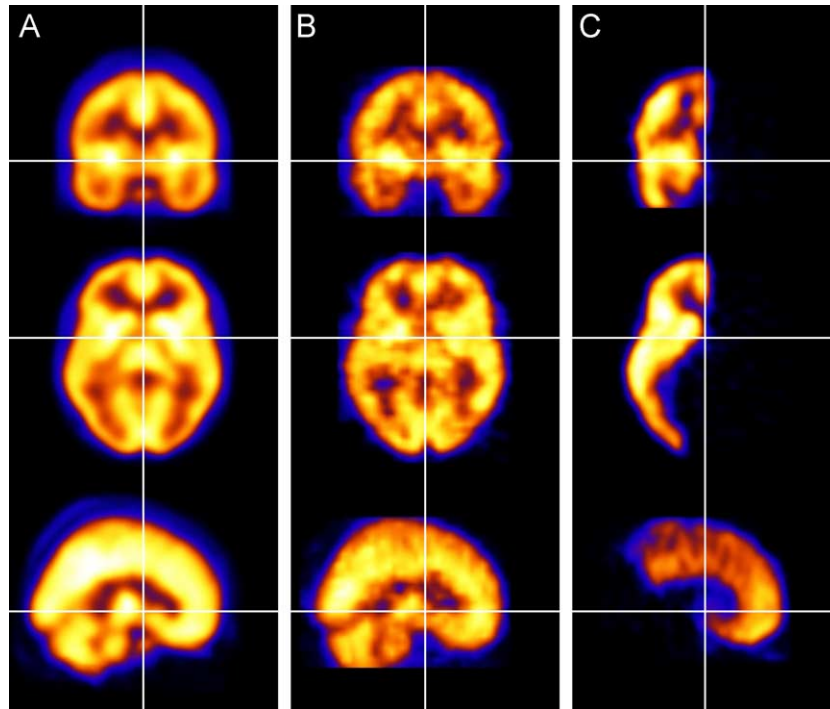


Fig. 3. (A) SPM Tc-99m-HMPAO SPECT template. (B) Spatially normalized basal SPECT image. (C) Spatially normalized IAP SPECT image using the transformation parameters obtained from the basal SPECT image in B.

patients with ICA stenosis. Before the carotid bypass surgery, patients with ICA or MCA stenosis showed significantly reduced cerebral perfusion in the involved ICA territory as compared with the age-matched healthy controls (two-tail t test, $P < 0.0005$). Mean and standard deviation of cerebral perfusion values obtained using extent probability maps in the involved ICA territory were $41.1 \pm 2.6 \text{ ml min}^{-1} \text{ g}^{-1}$ in patients and $43.5 \pm 1.7 \text{ ml min}^{-1} \text{ g}^{-1}$ in healthy controls. In patients, the cerebral perfusion reserve was $-10.9 \pm 6.3\%$ (-20.1% to -0.6%).

After the carotid bypass surgery, the basal cerebral perfusion in the ipsilateral ICA territory increased by $6.2 \pm 7.8\%$ (range: -6.7% – 17.1%) and cerebral perfusion reserve by $4.6 \pm 5.3\%$ (range: -3.2% – 12.8%).

Discussion

The anatomical standardization of IAP SPECT images is the most critical procedure involved in the generation of the ICA probabilistic maps. To perform anatomical standardization, IAP SPECT images were coregistered to the basal SPECT and transformed into a standard space using the spatial normalization parameters obtained from basal SPECT images. Two intensity-based automatic algorithms (Friston et al., 1995; Maes et al., 1997) for the image registration did not provide acceptable results: After image registration, IAP SPECT images were transformed so that the hemisphere of the brain shown in the IAP SPECT images was positioned in the center of the brain in basal SPECT images. These results had been expected to some extent since they had very different activity distributions. Although surface-based algorithms, which minimize the distance between the surfaces of brain, could be considered useful for the automatic registration of these images, a spherical or an ellipsoid-like outer surface shape of the ICA territory

in IAP SPECT images may have resulted in low rotation angle accuracies for image registration (Borgefors, 1998; Pelizzari et al., 1989). Estimation of the rotation angle with respect to the longest axis of the brain (the line that passes through the frontal and occipital poles) would be most inaccurate because of the limited cerebellar activity in the IAP SPECT images, which give brain surface in coronal slices a round shape. Another pitfall associated with a surface-based algorithm is the possibility of introducing errors during the extraction of the brain surface from the SPECT images. Since the signal to noise ratio is lower and the background activity from the skull, scalp, and soft tissues is higher in basal SPECT images than in IAP SPECT images, a brain surface extracted from basal SPECT will be less accurate and larger if the same criteria (i.e., threshold level) are used for the surface extraction.

User-interactive manual registration of the images by an experienced nuclear physician using a program specifically designed for this purpose would be the most practical solution in this case. The FIRE program used in the present study was developed to provide an efficient ways of image registration using both the automatic and manual method as explained in Materials and Methods. Validation of the accuracy of the manual registration using this program would be necessary, although we believe that this method was robust, reproducible, and accurate.

ICA probability maps in this study represent regional cerebral blood distributions via ICA. The extent probabilistic maps for ICA generated using population data delineated the brain regions that are supplied vascular flow by ICA. The regions in the anterior brain part showed little individual variation. However, in the medial temporal area and the posterior part of the brain including posterior cingulate cortex, and temporo-occipital cortex, the extent of ICA territory varied among individuals. Microanatomical studies showed the origin of the arteries supplying anterior

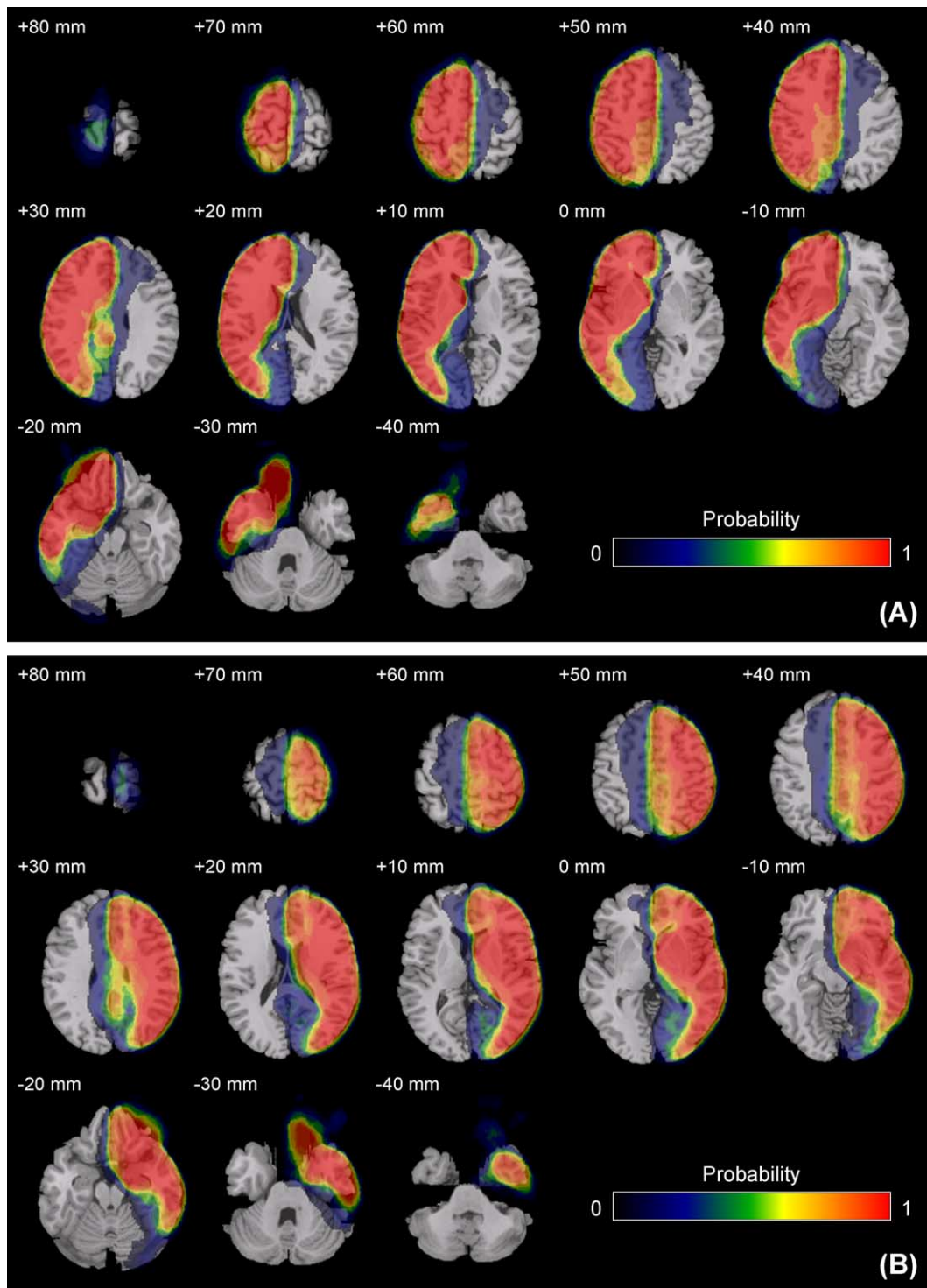


Fig. 4. Extent probabilistic maps of blood supply from the ICA, superimposed on an SPM T1 MRI template. (A) Left ICA map. (B) Right ICA map.

hippocampus, and uncus was mixed and included the anterior choroidal artery (AChA) branched from ICA and posterior cerebral artery (PCA) (Erdem et al., 1993; Huther et al., 1998; Muller and Shaw, 1965). In addition, many anastomoses originated from the AChA and PCA were found among the arteries in these regions (Huther et al., 1998). It was also shown that the temporo-occipital area was supplied blood from posterior temporal artery through MCA or lateral branch of PCA (Salamon and Huang, 1976;

Waddington, 1974). This variability was reflected in the extent probabilistic maps for ICA developed in this study.

Perfusion probabilistic maps represent the magnitude distribution of cerebral perfusion in addition to the vascular territory. The cortical arterial blood supply from the ICA was high in the insular, anterosuperior region of the temporal area and in the middle and inferior frontal gyrus, which may be due to the supply of blood from the inferior and superior divisions of the MCA, respectively.

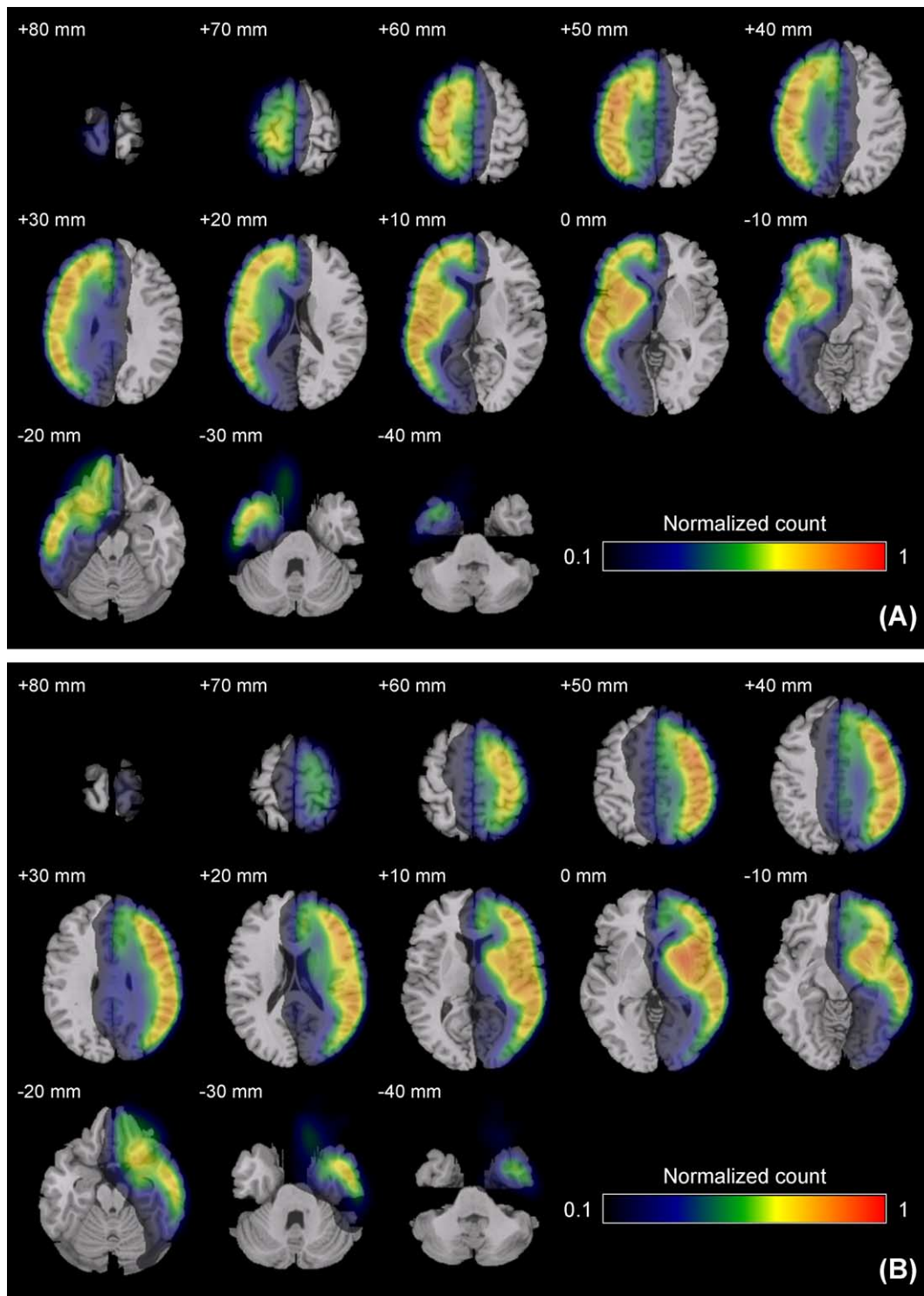


Fig. 5. Perfusion probabilistic maps of blood supply from the ICA, superimposed on an SPM T1 MRI template. (A) Left ICA map. (B) Right ICA map.

All medial cortical structures of the cerebral cortex, including the medial frontal gyrus, the cingulate gyrus, and the medial part of the sensory motor cortex, which are supplied with blood from anterior cerebral artery (ACA), showed an intermediate magnitude of blood supply from the ICA. The contralateral medial frontal lobe showed low, but significant magnitude, which may represent blood supply via the anterior communicating artery from the ICA of the

contralateral hemisphere. Of the subcortical structures, the basal ganglia were found to have the highest likelihood of being supplied by the ICA. However, the caudate nucleus showed a lower probability of blood supply from ICA than the other striatal structures. ICA probability maps showed a low supply probability for medial temporal structures, and this lower probability in the inferior, medial temporal structures represent mixed supply for

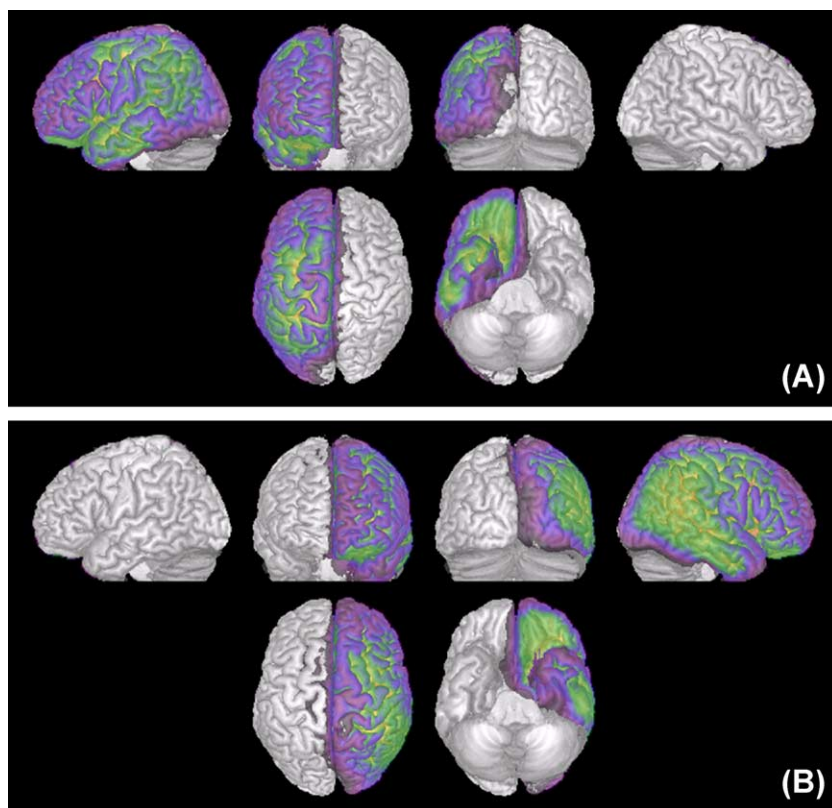


Fig. 6. Perfusion probabilistic maps of blood supply from the ICA, superimposed on the surface of an SPM T1 MRI template. (A) Left ICA map. (B) Right ICA map.

these regions from ICA and posterior circulation (de Silva et al., 1999; Hong et al., 2000; Jeffery et al., 1991; Kim et al., 1999, 2000).

The extent probabilistic maps of ICA territory can be used to define functional standard volumes of interest (VOI) for the assessment of the cerebral perfusion images of patients with ischemic cerebral artery disease. The patency of grafted vessels and of revascularized stenosed arteries can be directly assessed by the carotid angiography. This modality is, however, too invasive to perform repetitively, and effective blood flow after surgery for revascularization might be discrepant with angiographic findings, which can only show structural patency or the collateral circulation. Regional radioactivity in brain perfusion SPECT shows effective cerebral perfusion, which is the sum-up of forward and collateral circulation altogether at the level of brain cells. The Tc-99m-HMPAO and Tc-99m-ECD brain perfusion SPECT scan with or without acetazolamide stress have been shown effective in the assessment of patients with an ischemic cerebral artery or a postoperative bypass function in ischemic arteries (Cikrit et al., 1992; Garai et al., 2002; Iwama et al., 1997; Lee et al., 2004; Vorstrup et al., 1986).

Quantification of the perfusion shown in these brain SPECT images using the ICA probabilistic maps provides more useful information for the assessment of cerebral artery disease. In this study, we examined the efficacy of carotid bypass surgery in patients with ICA (and MCA) stenosis as a preliminary ICA probabilistic map application. Changes in cerebral perfusion and perfusion reserve observed using the ICA maps well represented the effective anterior cerebral circulation via the bypass graft after the operations.

The ICA probabilistic maps developed in this study have some limitations. First, the IAP SPECT images of patients with medial temporal lobe epilepsy were used to create the maps. Data from healthy subjects would have been useful but ethically inappropriate due to the possible morbidity during the procedure. The use of data from medial temporal lobe epilepsy patients might have resulted in an underestimation of ICA supply in the medial temporal regions. However, we believe that the use of this data can be justified by the following reason. Some medial temporal structures, such as the amygdala, uncus, and the anterior hippocampus, were found to be mainly supplied by the ICA (Kim et al., 1999; Marinkovic et al., 1991). Other areas in the medial temporal region, the posterior two thirds of the hippocampus, were found to be perfused by the posterior circulation in most subjects (Marinkovic et al., 1992; Muller and Shaw, 1965). Hypoperfusion related with the epileptogenic focus appears primarily in this region. The least distribution of HMPAO uptake in medial temporal structures matched the areas reported in the literature. We also could not find any report in the literature that single pass extraction is lower in epileptogenic tissues though it might be so theoretically. Thus, we believe that the influence of pathologic hypoperfusion on the ICA probabilistic maps is not expected to be significant.

Another possible limitation of this study is the use of sodium amobarbital, which can induce hypoperfusion (Kim et al., 1999). However, the injection of the Tc-99m-HMPAO as a mixture with sodium amobarbital did not allow enough time for sodium amobarbital to induce hypoperfusion as in intravenous SPECT during amobarbital test. Moreover, once trapped in the brain

tissue, back diffusion of Tc-99m-HMPAO is influenced by the cerebral blood flow. If cerebral blood flow is lowered by the amobarbital effects, back diffusion of Tc-99m-HMPAO will be reduced and net uptake will be increased. Thus, the effect of sodium amobarbital on the distribution of Tc-99m-HMPAO in the IAP SPECT is likely to be negligible.

Acknowledgments

This work was supported in part by the Korean Ministry of Science and Technology and in part by BK21 Human Life Sciences.

References

- Amunts, K., Zilles, K., 2001. Advances in cytoarchitectonic mapping of the human cerebral cortex. *Neuroimaging Clin. N. Am.* 11, 151–169.
- Baird, A.E., Donnan, G.A., Austin, M.C., Fitt, G.J., Davis, S.M., McKay, W.J., 1994. Reperfusion after thrombolytic therapy in ischemic stroke measured by single-photon emission computed tomography. *Stroke* 25, 79–85.
- Baird, A.E., Austin, M.C., McKay, W.J., Donnan, G.A., 1997. Sensitivity and specificity of 99mTc-HMPAO SPECT cerebral perfusion measurements during the first 48 hours for the localization of cerebral infarction. *Stroke* 28, 976–980.
- Bamford, J., Sandercock, P., Dennis, M., Burn, J., Warlow, C., 1991. Classification and natural history of clinically identifiable subtypes of cerebral infarction. *Lancet* 337, 1521–1526.
- Borgefors, G., 1998. Hierarchical chamfer matching: a parametric edge matching algorithm. *IEEE Trans. Pattern Anal. Mach. Intell.* 10, 849–865.
- Camargo, E.E., 2001. Brain SPECT in neurology and psychiatry. *J. Nucl. Med.* 42, 611–623.
- Chang, L.T., 1978. A method of attenuation correction in radionuclide computed tomography. *IEEE Trans. Nucl. Sci.* 25, 638–643.
- Cikrit, D.F., Burt, R.W., Dalsing, M.C., Lalka, S.G., Sawchuk, A.P., Waymire, B., Witt, R.M., 1992. Acetazolamide enhanced single photon emission computed tomography (SPECT) evaluation of cerebral perfusion before and after carotid endarterectomy. *J. Vasc. Surg.* 15, 747–753.
- Collins, L., Holmes, C., Peters, T.M., Evans, A.C., 1995. Automatic 3-D model-based neuroanatomical segmentation. *Hum. Brain Mapp.* 3, 190–208.
- de Silva, R., Duncan, R., Patterson, J., Gillham, R., Hadley, D., 1999. Regional cerebral perfusion and amygdala distribution during the Wada test. *J. Nucl. Med.* 40, 747–752.
- Erdem, A., Yasargil, G., Roth, P., 1993. Microsurgical anatomy of the hippocampal arteries. *J. Neurosurg.* 79, 256–265.
- Evans, A.C., Collins, D.L., Mills, S.R., Brown, E.D., Kelly, R.L., Peters, T.M., 1993. 3D statistical neuroanatomical models from 305 MRI volumes. *Proc. IEEE-Nuclear Science Symposium and Medical Imaging Conference*, pp. 1813–1817.
- Foley, J.D., Van Dam, A., Feiner, S.K., Hughes, J.F., 1996. *Computer Graphics: Principles and Practice*. Addison-Wesley Publishing Company, Inc., Boston.
- Friston, K.J., Ashburner, J., Frith, C.D., Poline, J.-B., Heather, J.D., Frackowiak, R.S.J., 1995. Spatial registration and normalization of images. *Hum. Brain Mapp.* 2, 165–189.
- Garai, I., Varga, J., Szomjak, E., Toth, C., Bank, J., Ficzere, A., Olvaszto, S., Galuska, L., 2002. Quantitative assessment of blood flow reserve using 99mTc-HMPAO in carotid stenosis. *Eur. J. Nucl. Med. Mol. Imaging* 29, 216–220.
- Giubilei, F., Lenzi, G.L., Di Piero, V., Pozzilli, C., Pantano, P., Bastianello, S., Argentino, C., Fieschi, C., 1990. Predictive value of brain perfusion single-photon emission computed tomography in acute ischemic stroke. *Stroke* 21, 895–900.
- Hong, S.B., Kim, K.W., Seo, D.W., Kim, S.E., Na, D.G., Byun, H.S., 2000. Contralateral EEG slowing and amobarbital distribution in Wada test: an intracarotid SPECT study. *Epilepsia* 41, 207–212.
- Huther, G., Dorfl, J., Van der Loos, H., Jeanmonod, D., 1998. Micro-anatomic and vascular aspects of the temporomesial region. *Neurosurgery* 43, 1118–1136.
- Iwama, T., Hashimoto, N., Takagi, Y., Tsukahara, T., Hayashida, K., 1997. Predictability of extracranial/intracranial bypass function: a retrospective study of patients with occlusive cerebrovascular disease. *Neurosurgery* 40, 53–59.
- Jeffery, P.J., Monsein, L.H., Szabo, Z., Hart, J., Fisher, R.S., Lesser, R.P., Debrun, G.M., Gordon, B., Wagner Jr., H.N., Camargo, E.E., 1991. Mapping the distribution of amobarbital sodium in the intracarotid Wada test by use of Tc-99m HMPAO with SPECT. *Radiology* 178, 847–850.
- Johansson, B., Norrving, B., Lindgren, A., 2000. Increased stroke incidence in Lund-Orup, Sweden, between 1983 to 1985 and 1993 to 1995. *Stroke* 31, 481–486.
- Kang, K.W., Lee, D.S., Cho, J.H., Lee, J.S., Yeo, J.S., Lee, S.K., Chung, J.K., Lee, M.C., 2001. Quantification of F-18 FDG PET images in temporal lobe epilepsy patients using probabilistic brain atlas. *NeuroImage* 14 (1 Pt. 1), 1–6.
- Kang, E., Lee, D.S., Lee, J.S., Kang, H., Hwang, C.H., Oh, S.H., Kim, C.S., Chung, J.K., Lee, M.C., Jang, M.J., Lee, Y.J., Morosan, P., Zilles, K., 2003. Developmental hemispheric asymmetry of interregional metabolic correlation of the auditory cortex in deaf subjects. *NeuroImage* 19, 777–783.
- Kim, B.G., Lee, S.K., Nam, H.W., Song, H.C., Lee, D.S., 1999. Evaluation of functional changes in the medial temporal region during intracarotid amobarbital procedure by use of SPECT. *Epilepsia* 40, 424–429.
- Kim, B.G., Lee, S.K., Kim, J.Y., Kang, D.W., Lee, W., Song, H., Lee, D.S., 2000. Interpretation of Wada memory test for lateralization of seizure focus by use of (99m) technetium-HMPAO SPECT. *Epilepsia* 41, 65–70.
- Kim, J.S., Lee, D.S., Lee, B.I., Lee, J.S., Shin, H.W., Chung, J.-K., Lee, M.C., 2002. Probabilistic anatomical labeling of brain structures using statistical probabilistic anatomical maps. *Korean J. Nucl. Med.* 6, 317–324.
- Laloux, P., Richelle, F., Jamart, J., De Coster, P., Laterre, C., 1995. Comparative correlations of HMPAO SPECT indices, neurological score, and stroke subtypes with clinical outcome in acute carotid infarcts. *Stroke* 26, 816–821.
- Lancaster, J.L., Woldorff, M.G., Parsons, L.M., Liotti, M., Freitas, C.S., Rainey, L., Kochunov, P.V., Nickerson, D., Mikiten, S.A., Fox, P.T., 2000. Automated Talairach atlas labels for functional brain mapping. *Hum. Brain Mapp.* 10, 120–131.
- Lassen, N.A., Andersen, A.R., Friberg, L., Paulson, O.B., 1988. The retention of [^{99m}Tc]-d,l-HM-PAO in the human brain after intracarotid bolus injection: a kinetic analysis. *J. Cereb. Blood Flow Metab.* 8, S13–S22.
- Lee, D.S., Lee, J.S., Kang, K.W., Jang, M.J., Lee, S.K., Chung, J.K., Lee, M.C., 2001. Disparity of perfusion and glucose metabolism of epileptogenic zones in temporal lobe epilepsy demonstrated by SPM/SPAM analysis on ¹⁵O water PET, [¹⁸F]FDG-PET, and [^{99m}Tc]-HMPAO SPECT. *Epilepsia* 42, 1515–1522.
- Lee, J.S., Ishii, K., Kim, Y.K., Sasaki, M., Lee, D.S., Chung, J.-K., Lee, M.C., 2002. Is the age-related decline of cerebral glucose metabolism due to the partial volume effect or not? *J. Nucl. Med.* 43, 66P (Abstract).
- Lee, H.Y., Paeng, J.C., Lee, D.S., Lee, J.S., Oh, C.W., Cho, M.J., Chung, J.K., Lee, M.C., 2004. Efficacy assessment of cerebral arterial bypass surgery using statistical parametric mapping and probabilistic brain atlas on basal/acetazolamide brain perfusion SPECT. *J. Nucl. Med.* 45, 202–206.

- Maes, F., Collignon, A., Vandermeulen, D., Marchal, G., Suetens, P., 1997. Multimodality image registration by maximization of mutual information. *IEEE Trans. Med. Imag.* 16, 187–198.
- Marinkovic, S.V., Milisavljevic, M.M., Vuckovic, V.D., 1991. Microvascular anatomy of the uncus and the parahippocampal gyrus. *Neurosurgery* 29, 805–814.
- Marinkovic, S., Milisavljevic, M., Puskas, L., 1992. Microvascular anatomy of the hippocampal formation. *Surg. Neurol.* 37, 339–349.
- Mead, G.E., Shingler, H., Farrell, A., O'Neill, P.A., McCollum, C.N., 1998. Carotid disease in acute stroke. *Age Ageing* 27, 677–682.
- Mazziotta, J.C., Toga, A.W., Evans, A., Fox, P., Lancaster, J., 1995. A probabilistic atlas of the human brain: theory and rationale for its development. *NeuroImage* 2, 89–101.
- Muller, J., Shaw, L., 1965. Arterial vascularization of the human hippocampus. *Arch. Neurol.* 13, 45–47.
- Pelizzari, C.A., Chen, G.T., Spelbring, D.R., Weichselbaum, R.R., Chen, C.T., 1989. Accurate three-dimensional registration of CT, PET, and/or MR images of the brain. *J. Comput. Assist. Tomogr.* 13, 20–26.
- Porter, T., Duff, T., 1984. Compositing digital images. *Proc. SIGGRAPH'84*, 18, 253–259.
- Rousset, O.G., Ma, Y., Evans, A.C., 1998. Correction for partial volume effects in PET: principle and validation. *J. Nucl. Med.* 39, 904–911.
- Salamon, G., Huang, Y.P., 1976. *Radiologic Anatomy of the Brain*. Springer Verlag, Berlin, Germany.
- Toga, A.W., Thompson, P.M., 2001. Maps of the brain. *Anat. Rec.* 265, 37–53.
- Vorstrup, S., Brun, B., Lassen, N.A., 1986. Evaluation of the cerebral vasodilatory capacity by the acetazolamide test before EC-IC bypass surgery in patients with occlusion of the internal carotid artery. *Stroke* 17, 1291–1298.
- Waddington, M.M., 1974. *Atlas of Cerebral Angiography with Anatomical Correlation*. Little Brown and Co., Boston.
- Watanabe, Y., Takagi, H., Aoki, S., Sassa, H., 1999. Prediction of cerebral infarct sizes by cerebral blood flow SPECT performed in the early acute stage. *Ann. Nucl. Med.* 13, 205–210.